Lysophosphatidylcholine Modulates Catalytically Important Motions of the Ca-ATPase Phosphorylation Domain†

Gregory W. Hunter, Diana J. Bigelow, and Thomas C. Squier*

Biochemistry and Biophysics Section, Department of Molecular Biosciences, University of Kansas, Lawrence, Kansas 66045-2106

Received October 7, 1998; Revised Manuscript Received January 14, 1999

ABSTRACT: Catalytically important motions of the Ca-ATPase, modulated by the physical properties of surrounding membrane phospholipids, have been suggested to be rate-limiting under physiological conditions. To identify the nature of the structural coupling between the Ca-ATPase and membrane phospholipids, we have investigated the functional and structural effects resulting from the incorporation of the lysophospholipid 1-myristoyl-2-hydroxy-*sn*-glycerol-3-phosphocholine (LPC) into native sarcoplasmic reticulum (SR) membranes. Nonsolubilizing concentrations of LPC abolish changes in fluorescence signals associated with either intrinsic or extrinsic chromophores that monitor normal conformational transitions accompanying calcium activation of the Ca-ATPase. There are corresponding decreases in the rates of calcium transport coupled to ATP hydrolysis, suggesting that LPC may increase conformational barriers associated with catalytic function. Fluorescence anisotropy measurements of the lipid analogue 1-(4-trimethylammoniumphenyl)-6-phenyl-1,3,5-hexatriene (TMA-DPH) partitioned into SR membranes indicate that LPC does not significantly modify lipid acyl chain rotational dynamics, suggesting differences in headgroup conformation between LPC and diacylglycerol phosphatidylcholines. Complementary measurements using phosphorescence anisotropy of erythrosin isothiocyanate at Lys^{464} on the Ca-ATPase provide a measure of the dynamic structure of the phosphorylation domain, and indicate that LPC restricts the amplitude of rotational motion. These results suggest a structural linkage between the cytosolic phosphorylation domain and the conformation of membrane phospholipid headgroups. Thus, changes in membrane phospholipid composition can modulate membrane surface properties and affect catalytically important motions of the Ca-ATPase in a manner that suggests a role for LPC generated during signal transduction.

Alterations in the phospholipid composition within biological membranes, including sarcoplasmic reticulum (SR), occur in response to a wide array of physiological and pathological conditions, and have been shown to modulate the function of both peripheral and integral membrane proteins (*1*−*6*). The physical basis for the functional regulation of active transport proteins by different membrane phospholipids has been suggested to result from changes in membrane physical properties (*7*−*14*). However, the inability to measure directly the influence of differences in membrane phospholipid composition on catalytically important protein structural changes has hindered a general understanding of the mechanisms responsible for the functional regulation of membrane proteins by their surrounding phospholipids. In this respect, the recent identification of global conformational changes that accompany calcium activation now permits an investigation of the physical mechanisms responsible for modulation of active transport function by membrane phospholipids (*15*−*17*).

Increases in the phosphoethanolamine (PE) content of reconstituted proteoliposomes containing the Ca-ATPase have previously been shown to correlate with increases in the amplitude of rotational dynamics of the phosphorylation domain and enhanced catalytic activity of the Ca-ATPase (*5*, *18*−*20*). Therefore, specific interactions between PE headgroups and selected amino acids (e.g., tryptophan) near the bilayer surface of the Ca-ATPase may enhance catalytic function as a result of the modulation of the structural coupling between the calcium binding sites located within the transmembrane helices in the bilayer and the nucleotide binding site in the cytosolic portion of the Ca-ATPase (*5*, *21*). Alternatively, differences in the average conformation of the phosphocholine and phosphoethanolamine headgroups within liquid crystalline membranes may modulate structural changes associated with the transport mechanism of the Ca-

† Supported by the National Institutes of Health (Grant GM46837).

* Correspondence should be addressed to Thomas C. Squier. Tel: (913)-864-4008. Fax: (913)-864-5321. E-mail: TCSQUIER@KUHUB.CC.UKANS.EDU.

[1] Abbreviations: ATP, adenosine 5-triphosphate; calcium green, 5*N*,*N*-[2-[2-[2-[bis(carboxymethyl)amino]-5-[[(2′,7′-dichloro-3′,6′-dihydroxy-3-oxospiro[isobenzofuran-1(3H),9′-[9H]xanthen]-5-yl)carbonyl]-amino]phenoxy]ethoxy]-4-nitrophenyl]-*N*-(carboxymethyl) glycine; CCCP, carbonyl cyanide 3-chlorophenyl hydrazone; $C_{12}E_9$, polyoxyethylene 9 lauryl ether; DOPE, dioleoylphosphatidyl ethanolamine; DOPC, dioleoylphosphatidylcholine; EGTA, ethylene glycol bis-(β-amino-ethyl ether) *N*,*N*,*N*′,*N*′-tetraacetic acid; Er-ITC, erythrosin 5-isothiocyanate; FURA-2, 1-[2-(5-carboxyazol-2-yl)-6-aminobenzofuran-5-oxyl]-2-(2-amino-5-methylphenoxy)ethane-*N*,*N*,*N*′,*N*′-tetraacetic acid; LPC, 1-myristoyl-2-hydroxy-*sn*-glycerol-3-phosphocholine; MOPS, 3-(*N*-morpholino) propane sulfonic acid; PC, phosphatidylcholine; PE, phosphatidylethanolamine; r_o, initial anisotropy; r_∞, residual anisotropy; S, order parameter; SR, sarcoplasmic reticulum; TMA-DPH, 1-(4-trimethylammoniumphenyl)-6-phenyl-1,3,5-hexatriene; $\langle\tau\rangle$, average fluorescence lifetime; ϕ, rotational correlation time.

10.1021/bi982392g CCC: $18.00
Published on Web 03/17/1999

ATPase as a result of differences in the electrostatic potential at the membrane surface (*22*−*26*). To clarify the structural linkage between membrane phospholipids and the Ca-ATPase, we have investigated the influence of the incorporation of the lysophosphatidylcholine 1-myristoyl-2-hydroxy-*sn*-glycerol-3-phosphocholine (LPC) into native SR membranes on Ca-ATPase function and dynamics. Lysophosphatidylcholines, in which the fatty acyl chain in the *sn*-2 position is selectively cleaved, are generated following activation of phospholipase A_2 (PLA_2) (*27*). Lysophospholipids have been implicated as downstream affecters in signal transduction, and are present at significant concentrations in cellular membranes during intracellular signaling and following a range of different pathological conditions that result in the activation of phospholipase A_2 (*28*, *29*). While the role of lysophosphatidylcholines in signal transduction remains unclear, their presence in membranes has been suggested to modulate the activity of many different peripheral and integral membrane proteins (*30*−*32*). Because phospholipase A_2 (PLA_2) activity in cardiac and neuronal tissues has been shown to be activated at elevated intracellular calcium levels (*30*, *32*), any decrease in Ca-ATPase activity may function to potentiate signal transduction cascades through the modulation of intracellular calcium homeostasis and to further accentuate imbalances in the rates of phospholipid degradation and repair. For example, within several minutes following induction of long-term potentiation in the brain, increased PLA_2 activity functions to selectively deplete membrane PC levels, resulting in a 4-fold decrease in PC and large increases in amounts of free fatty acids (*30*, *32*). However, under pathophysiological conditions LPC levels become sufficiently high so as to disrupt ion gradients and to be primary mechanisms of cell death (*32*). These observations suggest that nonsolubilizing concentrations of lysophosphatidylcholines are physiologically relevant, and that under these conditions that cell viability is maintained. To identify the influence of nonsolubilizing concentrations of lysophosphatidylcholines in modulating Ca-ATPase function, we investigated structural changes involving both the Ca-ATPase and surrounding lipids in native membranes using both phosphorescence anisotropy measurements of Er-ITC covalently bound to Lys_{464} in the phosphorylation domain of the Ca-ATPase, and fluorescence anisotropy measurements of TMA-DPH partitioned into membrane lipids. LPC induces structural changes of the Ca-ATPase that are found to correlate with catalytic activity, suggesting a physiologically important role for lipid−protein interactions in modulating calcium transport function.

EXPERIMENTAL PROCEDURES

Materials. KCl was purchased from Research Organics (Cleveland, OH). Sucrose, TRIS (free base), and MOPS [3-(*N*-morpholino) propane sulfonic acid] were obtained from Fisher Scientific (Pittsburgh, PA). $CaCl_2$ standard solution was from VWR (St. Louis, MO). A23187, ammonium molybdate, ATP (disodium salt), isomer II of Er-ITC (erythrosin 5-isothiocyanate), isomer I of fluorescein 5-isothiocyanate (FITC), and EGTA were from Sigma (St. Louis, MO). The proton ionophore carbonyl cyanide 3-chlorophenyl hydrazone (CCCP) was obtained from Fluka Chemical Corp. (Ronkonkoma, NY). 2-(3-(Diphenylhexatrienyl) propanoyl)-1-hexadecanoyl-*sn*-glycero-3-phosphocholine (TMA-DPH) and 1-myristoyl-2-hydroxy-*sn*-glycerol-3-phosphocholine (LPC) were obtained from Avanti Polar Lipids (Alabaster, AL). 1-[2-(5-Carboxyazol-2-yl)-6-aminobenzofuran-5-oxyl]-2-(2-amino-5-methylphenoxy)ethane-*N*,*N*,*N*′,*N*′-tetraacetic acid (FURA-2) and *N*-[2-[2-[2-[bis(carboxymethyl)amino]-5-[[(2′,7′-dichloro-3′,6′-dihydroxy-3-oxospiro[isobenzofuran-1(3H),9′-[9H]xanthen]-5-yl)carbonyl]amino]phenoxy]ethoxy]-4-nitrophenyl]-*N*-(carboxymethyl) glycine (calcium green-5N) were purchased from Molecular Probes, Inc. (Eugene, OR). SR membranes were isolated from rabbit fast-twitch skeletal muscle, essentially as previously described (*33*). SR lipids were extracted as previously described (*34*−*35*). All samples were stored in 20 mM MOPS (pH 7.0) and 0.3 M sucrose at −70 °C.

Derivatization of Samples with Optical Probes. Er-ITC was covalently bound to Lys_{464} on the Ca-ATPase at a stoichiometry of approximately one nanomole of Er-ITC bound per milligram of SR membranes, as previously described in detail (*36*). Lys_{515} within the Ca-ATPase was labeled with FITC as previously described (*37*). TMA-DPH was partitioned into membranes for measurements of phospholipid acyl chain rotational dynamics at a concentration of 0.5% (mol/mol).

Enzymatic Activity Assays. Protein concentrations were measured using the Amidoschwarz protein assay using nitrocellulose paper and Amidoblack stain (*38*). Free calcium concentrations were directly measured using either FURA-2 or calcium green, whose respective association constants for calcium were measured to be 186 ± 3 nM and 3.0 ± 0.4 μM under these experimental conditions (*39*). Calcium uptake was measured essentially as previously described (*40*) and was initiated by the addition of 1 mM ATP to a calcium-buffered solution containing 200 mM MOPS (pH 7.0), 0.1 mM KCl, 5 mM $MgCl_2$, 0.5 μM CCCP, 5 mM calcium oxalate, 2 mM EGTA, and sufficient calcium to yield a free calcium concentration equal to 2 μM. Fluorescence changes in calcium green-5N were used to measure changes in free calcium concentration, permitting the calculation of the total amount of calcium uptake using the following relationship:

$$[Ca^{2+}]_{uptake} = [Ca^{2+}]_{free}\left[1 + \frac{K_{EGTA}[EGTA]}{1 + K_{EGTA}[Ca^{2+}]_{free}}\right] \quad (1)$$

where the association constant for calcium binding to EGTA (K_{EGTA}) is 2.5×10^6 M^{-1} (*40*). Calcium-dependent rates of ATP hydrolysis were measured as an ammonium molybdate complex of phosphate at 25 °C (*41*) and involved 0.1 mg/mL SR vesicles in a medium containing 200 mM MOPS (pH 7.0), 100 mM KCl, 5 mM $MgCl_2$, 1 mM ATP, 6 μM A23187, 0.5 μM CCCP, 2 mM EGTA, and sufficient calcium to yield the indicated free calcium concentration.

The calcium-dependent activation of the Ca-ATPase was fit to a model involving the cooperative binding of two ligands:

$$\text{ATPase Activity} = \frac{K_1[Ca^{2+}]_{free} + 2K_2[Ca^{2+}]^2_{free}}{2(1 + K_1[Ca^{2+}]_{free} + K_2[Ca^{2+}]^2_{free})} \quad (2)$$

where K_1 is the macroscopic equilibrium constant, and corresponds to the sum of the intrinsic equilibrium constants

(k_1 and k_2) associated with calcium activation of the Ca-ATPase; and K_2 is the intrinsic equilibrium constant for calcium activation and corresponds to the product of equilibrium constants ($k_1k_2k_c$) (*42*). This assessment of calcium activation permits a determination of the cooperativity (i.e., k_c) between high-affinity calcium binding sites in the Ca-ATPase.

Fluorescence Measurements. Excitation of TMA-DPH involved the 364 nm line from a Coherent Innova 400 argon ion laser (Santa Clara,CA) and the fluorescence emission were detected by using a Schott GG400 long-pass filter using an ISS K2 frequency domain fluorometer, as described previously (*43*). FITC was excited at 442 nm and emission was detected by using a Schott GG495 long-pass filter. Excitation of FURA-2 and calcium green-5N were respectively at 345 and 488 nm; emission was monitored at 510 and 530 nm using a Spex FluoroMax-2 (Edison, NJ).

Phosphorescence Measurements. Er-ITC was covalently bound to Lys_{464} on the Ca-ATPase at a stoichiometry of approximately 0.2 mol of Er-ITC bound/mol of Ca-ATPase, essentially as previously described (*36*). Er-ITC derivatized SR vesicles (0.1 mg/mL) were excited using approximately 1 mW of 514 nm modulated light from an argon ion laser (Coherent Corp., Palo Alto, CA), and the phosphorescence emission was collected after a Schott RG697 long-pass filter essentially as previously described (*17*). Prior to the measurement of phosphorescence, the concentration of dissolved oxygen in a 3 mL sealed cuvette was reduced enzymatically by the addition of 17 mM glucose, 3 units of glucose oxidase activity, and 30 units of catalase activity, and subsequent incubation in the dark for at least 5 min (*17, 44*).

Analysis of Fluorescence or Phosphorescence Intensity and Anisotropy Decays. Phosphorescence intensity or anisotropy decays were fit to a sum of exponentials using the method of nonlinear least-squares using explicit expressions that permit the calculation of the lifetime components relating to a multiexponential decay (α_i and τ_i; refs *45*−*46*), where

$$\Phi_{\phi\omega} = \arctan\frac{N_\omega}{D_\omega} \quad \text{and} \quad m_{\phi\omega} = \sqrt{N_\omega^{\,2} + D_\omega^{\,2}} \qquad (3)$$

N_ω and D_ω are specific mathematical transforms that relate the measured phase shift (ϕ_ω) and modulation (m_ω) to the lifetime components associated with the excited-state intensity decay of the chromophore. Alternatively, appropriate expressions have been derived that permit determination of the initial anisotropy in the absence of rotational diffusion (r_0), the rotational correlation times (ϕ_i), and the amplitudes of the total anisotropy loss associated with each rotational correlation time ($r_0\ g_i$). The derivation and application of these expressions have previously been described in detail (*43*, *46*−*48*).

In the case of TMA-DPH partitioned into SR membranes, these transforms (i.e., N_ω and D_ω) can be readily modified to take into account a heterogeneous population of membrane phospholipids that undergo slow exchange during the excited-state lifetime of TMA-DPH, which can be approximated by two populations of structural conformers corresponding to (i) phospholipids not in contact with the Ca-ATPase with a structure analogous to lipids in vesicles made from SR lipids (i.e., bulk lipid) or (ii) protein-associated lipids (PALs) in contact with the Ca-ATPase, where

$$N_{\omega_i} = f_{\mathrm{PALS}_i} N_{\mathrm{PALS}_i} + (1 - f_{\mathrm{PALS}_i}) N_{\mathrm{BULK-LIPID}} \qquad (4)$$

and

$$D_{\omega_i} = f_{\mathrm{PALS}_i} D_{\mathrm{PALS}_i} + (1 - f_{\mathrm{PALS}_i}) D_{\mathrm{BULK-LIPID}} \qquad (5)$$

Previous spin-label EPR measurements indicate that the Ca-ATPase modifies the rotational dynamics of 43% of membrane phospholipids in SR membranes, which correspond to the PALs (*49*). Therefore, an independent measurement of the individual lifetime components and associated amplitudes relating to TMA-DPH in membranes made from extracted SR lipids (i.e., α_i and τ_i) provides a measurement of the bulk lipid, and permits one to recover the average lifetime parameters (i.e., α_i and τ_i) and rotational dynamics (i.e., ϕ_1 and S) associated with the PALs. The parameter values are determined using the method of nonlinear least-squares in which the reduced chi-squared (i.e., χ_R^2) is minimized. A comparison of χ_R^2 provides a quantitative measurement of the adequacy of different assumed models to describe the data (*47*). Data were fit using either the Globals software package (University of Illinois, Urbana-Champaign) or using the program Mathcad 6.0 (MathSoft Inc., Cambridge, MA). The reported experimental uncertainties associated with each parameter were determined from a global analysis of the respective error surfaces, using the F statistic associated with one standard deviation (*47*). To simplify the presentation of the data, in cases where the error surfaces are not symmetrical the reported errors represent the maximal variance obtained from the error analysis. Unless otherwise indicated, data were analyzed using frequency-independent errors in the phase and modulation that were assumed to be 0.2° and 0.01, respectively.

RESULTS

Influence of Lysophosphatidylcholine on Bilayer Structure. Lysophosphatidylcholines (LPC) are involved in normal intracellular signaling; however, at sufficiently high concentrations lysophosphatidylcholines act to disrupt biological membranes resulting in increased membrane permeability and modified interactions between membrane proteins that can result in cell death (*29, 32*). Therefore, it is essential to distinguish LPC concentrations at which SR membrane integrity is disrupted from lower nonsolubilizing concentrations where cell viability is expected to be preserved.

To detect alterations in protein−protein associations resulting from LPC solubilization of the membrane, we have monitored the loss of resonance energy transfer (RET) between FITC chromophores bound to Lys_{515} near the nucleotide binding site. Increased RET between identical chromophores (homotransfer) was monitored with steady-state polarization (P), which provides a sensitive means to assess protein−protein associations (*37, 50*−*56*). We find that increasing concentrations of LPC result in essentially no change in P for LPC concentrations below 0.2 mg/mg of SR protein (0.02 mg/mL), followed by a progressive increase in P from 0.26 to 0.48 upon further increasing the concentration of LPC (Figure 1). These data agree with light scattering measurements used to measure vesicle integrity through changes in turbidity. Thus, solubilization of SR membranes only occurs at concentrations above 0.2 mg of LPC/mg of

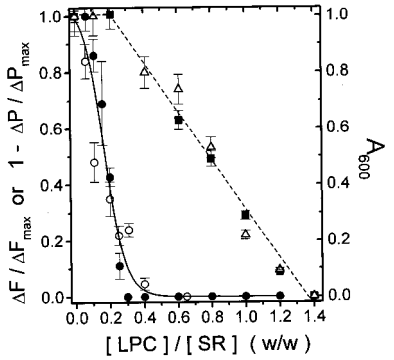

FIGURE 1: Modulation of Calcium-Dependent Structural Changes by LPC. Influence of LPC on calcium-dependent fluorescence intensity changes associated with intrinsic tryptophans (●) or FITC covalently bound to Lys_{515} (○), which respectively increase 4% and decrease 8% upon calcium activation. Membrane integrity was assessed using light scattering at 600 nm (△) or changes in the fluorescence polarizarization of FITC (■) resulting from fluorescence resonance energy transfer (FRET) to detect alterations in the spatial arrangement of Ca-ATPase polypeptide chains with respect to one another. Experimental conditions involved 0.1 mg/mL SR in 50 mM MOPS (pH 7.0), 80 mM KCl, 5 mM $MgCl_2$, and 0.1 mM EGTA. Calcium activation was assayed after the addition of 0.2 mM $CaCl_2$. FITC and tryptophan were respectively excited using 490 and 298 nm light, and the resulting fluorescence was detected at 520 nm and using a Schott WG-335 long-pass filter, respectively.

SR protein. Furthermore, since significant changes in the conformation of the nucleotide binding site would be expected to alter FITC probe orientation and thus P (*57*), these results further indicate that Ca-ATPase structure is relatively unaffected at these lower LPC concentrations.

The partition coefficient for lysophospholipid incorporation into membranes has previously been determined to be 1.1×10^6 (*58*), indicating that under these experimental conditions 98% of the added LPC is incorporated into the SR membrane. To avoid nonspecific effects that may involve alterations in the integrity of the SR membrane, we have chosen an LPC concentration of 0.02 mg/mL to investigate how LPC incorporation into the SR membrane modifies function. The addition of 0.02 mg/mL LPC into SR membranes (0.1 mg/mL) corresponds to about 35 mol of LPC/mol of Ca-ATPase, or approximately 24% of the total phospholipids based on typical molar ratios of 145 phospholipids/mol of Ca-ATPase in native SR membranes (*49*). Since PC and PE respectively represent 58% ± 10% and 16% ± 4% of the total phospholipid content of SR membranes (*59*), the incorporation of 35 mol of LPC/mol of Ca-ATPase results in a 7% increase in the relative concentration of PC headgroups and a corresponding 3% decrease in the molar fraction of PE headgroups. This small alteration in the relative amounts of PC and PE is expected to have little influence on membrane function (*5*).

Measurement of Calcium Transport and ATP Hydrolysis Rates. To identify the functional consequences of nonsolubilizing concentrations of LPC on the Ca-ATPase, we have compared rates of both calcium uptake and ATP hydrolysis for native SR membranes before and after the addition of 0.2 mg of LPC/mg of SR protein. At this nonsolubilizing concentration, LPC incorporation results in a small but reproducible decrease in function of the Ca-ATPase, resulting in a 16% ± 8% decrease in the maximal rate of calcium uptake and a 17% ± 9% decrease in the rate of ATP hydrolysis (Table 1, Figure 2). Furthermore, the calcium

Table 1: Influence of LPC on Catalytic Function of Ca-ATPase in Native SR Vesicles[a]

[LPC]/[SR] (mass/mass)	ATPase activity[b] (μmol of P_i mg^{-1} min^{-1})	calcium transport activity[c] (μmol of Ca^{2+} mg^{-1} min^{-1})	coupling ratio[d] (Ca^{2+} transported/ATP hydrolyzed)
0	3.0 ± 0.2	5.6 ± 0.2	1.9 ± 0.1
0.2	2.5 ± 0.2	4.7 ± 0.4	1.9 ± 0.2

[a] Temperature was 25 °C and buffer conditions are as indicated in the legend to Figure 2. [b] Initial rates of ATP hydrolysis. [c] Initial rates of calcium uptake. [d] Coupling ratios are obtained by dividing the calcium uptake rate by the ATPase activity.

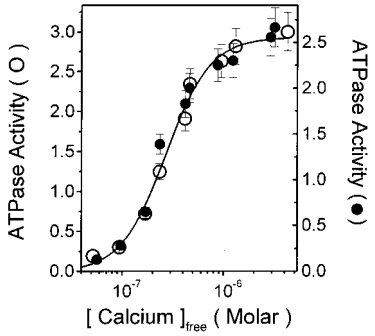

FIGURE 2: Calcium Dependence of the Activation of the Ca-ATPase. Samples correspond to either native SR membranes (○, left abscissa) or following the addition of 0.2 mg of LPC per milligram of SR protein (●; right abscissa). The line represents the experimental fit to eq 2 (see Experiment Procedures) where $\Delta G_1 = -6.9 \pm 1.2$ kcal/mol; $\Delta G_2 = -17.9 \pm 0.1$ kcal/mol; and $\Delta G_c = -5.0 \pm 1.2$ kcal/mol. Maximal rates of ATP hydrolysis at saturating calcium are also listed in Table 1. Calcium-dependent rates of ATP hydrolysis were measured using 0.1 mg/mL SR at 25 °C in the presence of 200 mM MOPS (pH 7.0), 0.1 M KCl, 5 mM $MgCl_2$, 1 mM ATP, 2 mM EGTA, 6 μM A23187, 0.5 μM CCCP, and sufficient $CaCl_2$ to yield the indicated free calcium concentrations. Free calcium concentrations were directly measured using FURA-2 and calcium green, whose respective binding affinities were measured to be 186 ± 3 nM and 3.0 ± 0.4 μM under these experimental conditions (*39*). Values for reconstituted samples represent the average of three independent determinations, and average errors were 6% of the indicated values.

gradient generated by the Ca-ATPase is maintained following the consumption of ATP irrespective of the presence of LPC (data not shown), ruling out nonspecific calcium leaks. LPC results in the same decrease in catalytic activity irrespective of the calcium concentration, indicating that there are no changes in apparent calcium affinity or in the cooperativity between the high-affinity calcium binding sites. Therefore, LPC modifies the rate of calcium transport involving catalytic steps following calcium activation.

Modulation of Ca-ATPase Structure by Membrane Phospholipids. The influence of LPC on structural transitions between enzymatic states involved in the transport cycle of the Ca-ATPase can be readily examined through measurements of calcium-dependent alterations in the steady-state fluorescence intensity of intrinsic chromophores (i.e., tryptophans) that are predominantly located near the bilayer surface or FITC covalently bound to Lys_{515} near the nucleotide binding cleft (*60*, *61*). These fluorescence signals reflect the long-range structural coupling between the high-affinity calcium binding sites located within the transmembrane helices and spatially distant nucleotide binding site(s) (*15*, *62*, *63*). Calcium activation induces a 3−4% increase in the intrinsic fluorescence of tryptophans and an 8% decrease in that of bound FITC (*60*, *64*−*66*). The addition

Table 2: Calcium-Dependent Changes in the Average Fluorescence Lifetimes of Tryptophan[a]

[LPC]/[SR] (mass/mass)	ligand	f_1	τ_1 (ns)	f_2	τ_2 (ns)	f_3	τ_3 (ns)	$\langle\tau\rangle$ (ns)	χ_R^2
0.0	+EGTA	0.026	0.2	0.26	2.1	0.71	5.0	4.1	0.6
		(0.003)	(0.1)	(0.04)	(0.1)	(0.04)	(0.2)	(0.3)	
	+calcuim	0.032	0.2	0.56	2.9	0.41	7.5	4.7	3.8
		(0.002)	(0.1)	(0.08)	(0.1)	(0.08)	(0.5)	(0.9)	
0.2	+EGTA	0.035	0.2	0.67	3.3	0.29	9	4.9	4.3
		(0.005)	(0.1)	(0.08)	(0.3)	(0.08)	(2)	(1.2)	
	+calcium	0.034	0.2	0.68	3.3	0.29	9	4.8	4.3
		(0.004)	(0.1)	(0.05)	(0.1)	(0.05)	(1)	(0.8)	

[a] Differential phase and modulation were collected at 23 frequencies between 7.5 and 200 MHz. Excitation was at 298 nm and emission was collected using WG-320 long-pass and Corning 7-51 interference filters. Experimental conditions involved 0.1 mg/mL SR in 50 mM MOPS (pH 7.0), 80 mM KCl, 5 mM $MgCl_2$, and 0.1 mM EGTA. When appropriate, 0.2 mM $CaCl_2$ or 20 μg/mL LPC was included in the buffer. Temperature was 25 °C.

Table 3: Calcium-Dependent Changes in the Rotational Dynamics of Tryptophan[a]

[LPC]/[SR] (mass/mass)	ligand	$\langle\tau\rangle$ (ns)	$g_1 r_0$	ϕ_1 (ns)	r_∞	χ_R^2
0.0	+EGTA	4.1	0.132	0.9	0.144	1.9
		(0.3)	(0.008)	(0.2)	(0.002)	
	+calcium	4.7	0.162	0.60	0.142	1.6
		(0.9)	(0.003)	(0.05)	(0.001)	
0.2	+EGTA	4.9	0.12	1.2	0.160	2.9
		(1.2)	(0.01)	(0.4)	(0.002)	
	+calcium	4.8	0.12	0.9	0.168	2.5
		(0.8)	(0.01)	(0.2)	(0.003)	

[a] Experimental conditions are as described in the legend to Table 2, where numbers in parentheses represent the standard deviation from two independent measurements. Parameter values are obtained from fitting the data to a sum of exponentials, as previously described (*47*, *67*).

of nonsolubilizing concentrations of LPC to native SR membranes results in progressive decreases that eventually abolish these calcium-dependent changes in fluorescence signals (Figure 1). The diminished calcium-dependent change in these fluorescence signals is analogous to previous results where alterations in the lipid environment surrounding the Ca-ATPase also have been shown to reduce these calcium-dependent changes in fluorescence intensity (*60*, *66*).

Lifetime and Rotational Dynamics of Tryptophan Side Chains. Changes in the average fluorescence intensity of the thirteen tryptophan residues in the Ca-ATPase could result from differences in phospholipid-induced changes in the environment of a minor fraction of tryptophan side chains, rather than reflecting global structural changes. In contrast, fluorescence lifetime decays require changes in the environment of the *majority* of the tryptophan side chains (*67*). We have, therefore, measured the frequency response of the tryptophan fluorescence in the presence and absence of added LPC (Table 2). In agreement with previous results, the intensity decay associated with tryptophan can, in all cases, be adequately described by a model involving three exponentials (*67*). Prior to the addition of LPC, calcium activation results in a shift in the frequency response to lower frequencies, consistent with the observed 4% enhancement in steady-state fluorescence intensity. The addition of nonsolubilizing concentrations of LPC abolishes the calcium-dependent shift in the frequency response of the fluorescence decay, and the calcium-dependent changes in both the fractional intensities and lifetime components of the tryptophan intensity decay are diminished (Table 2). Thus, the loss of the calcium-dependent changes in the steady-state fluorescence intensity of tryptophan is a reflection of diminished global conformational changes involving the majority of the membrane-embedded tryptophans upon addition of LPC (Table 2; Figure 1).

Similarly, calcium-dependent changes in tryptophan rotational dynamics are abolished upon partitioning nonsolubilizing concentrations of LPC into these SR membranes (Table 3). These calcium-dependent changes in tryptophan rotational dynamics have previously been suggested to reflect steric differences in side chain packing that accompany the reorientation of the transmembrane helices (*67*). The reduced calcium sensitivity to changes in both the lifetime and rotational dynamics of tryptophans is consistent with stabilization of the Ca-ATPase in a state analogous to calcium activation following incorporation of LPC (*60*, *66*). Alternatively, LPC may stabilize the Ca-ATPase in a conformation different from that observed in native SR membranes (Tables 2 and 3).

Phosphorescence Anisotropy Measurements of Protein Rotational Dynamics. To investigate the influence of LPC on catalytically important motions that have been implicated as important to the transport activity of the Ca-ATPase (*5*, *17*), we have measured the rotational dynamics of the phosphorylation domain covalently modified with Er-ITC. Er-ITC has previously been shown to selectively modify Lys_{464} within the phosphorylation domain of the Ca-ATPase, without interfering with the catalytic activity associated with the high-affinity nucleotide binding site (*36*). Furthermore, frequency domain measurements of phosphorescence anisotropy have been shown to accurately measure membrane protein rotational dynamics, providing equivalent resolution to time domain measurements while avoiding artifacts from fluorescence and light scattering (*5*, *17*). Thus, dynamic structural changes involving the phosphorylation domain of the Ca-ATPase that result from alterations in lipid−protein interactions can be directly measured using frequency domain phosphorescence spectroscopy. In addition, these measurements permit the resolution of alterations in either interactions between Ca-ATPase polypeptide chains or changes in the membrane fluidity, since the rate of overall rotational motion of the Ca-ATPase with respect to the membrane normal has been shown to be sensitive to both the size of the Ca-ATPase and the viscosity of the membrane bilayer (*17*, *68*−*70*).

The average phosphorescence lifetime of Er-ITC covalently bound to the Ca-ATPase was 200 ± 50 μs irrespective of the presence of LPC (data not shown). This lifetime is sufficiently long to permit the measurement of internal domain motions and the overall rotational motion of the Ca-ATPase with respect to the membrane normal (*17*). Resolution of the rotational dynamics of the Ca-ATPase involved the measurement of the differential phase and modulated anisotropy between 0.1 and 20 kHz. Addition of LPC results in a shift in the frequency response of the modulated anisotropy and differential phase to lower frequencies (Figure 3), indicating decreased rotational mobility. Irrespective of the addition of LPC, the frequency domain anisotropy data can be adequately described by a model involving a sum of two exponentials and a residual anisot-

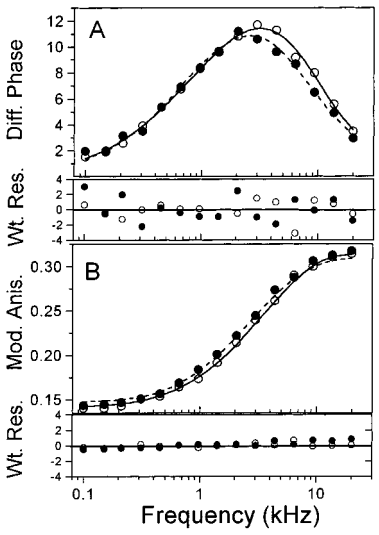

FIGURE 3: Influence of LPC on the Rotational Dynamics of the Ca-ATPase. Differential phase (A) and modulated anisotropy (B) data and corresponding multiexponential fits for native SR (○, solid line) and following the addition of 0.2 mg of LPC per milligram of SR protein (●, dashed line). Weighted residuals are shown below their respective data sets, and correspond to the difference between the experimental and calculated least-squares fit to the data normalized by frequency-independent experimental errors that were assumed to be 0.2° and 0.01 for the differential phase and modulated anisotropy, respectively. The χ^2_R values are 0.8 (solid lines) and 1.7 (dashed lines). Experimental conditions involved 0.1 mg/mL SR in 200 mM MOPS (pH 7.0), 0.1 M KCl, 5 mM $MgCl_2$, 2 mM EGTA, and 1.65 mM $CaCl_2$; the free calcium concentration was approximately 2 μM.

ropy, as shown by the randomly weighted residuals. A consideration of the temperature dependence of the rotational dynamics of Er-ITC bound to the Ca-ATPase, and comparison of the Arrhenius activation energies with those associated with lipid dynamics (measured using TMA-DPH), indicate that the measured rotational correlation times correspond to the rotational motion of the phosphorylation domain ($\phi_1 \approx 6$ μs) and the overall rotational motion of the Ca-ATPase with respect to the membrane normal ($\phi_2 \approx 170$ μs) (*17*). These rotational correlation times are sensitive to changes in the average structure of either the phosphorylation domain, alterations in the interactions between Ca-ATPase polypeptide chains, or changes in membrane fluidity (*69*, *71*). Likewise, the residual anisotropy (r_∞) is sensitive to differences in the average orientation of the phosphorylation domain relative to the membrane normal (*68*, *70*). A consideration of the fitting parameters for native SR and following incorporation of LPC indicates that LPC primarily acts to reduce the amplitude (g_1) associated with domain motion (ϕ_1); no significant changes in the rotational correlation times or residual anisotropies are observed (Table 4). Thus, these results imply that LPC does not directly modify the average conformation of the phosphorylation domain, interactions between Ca-ATPase polypeptide chains, or membrane fluidity. Rather LPC modulates catalytically important dynamic structural changes of the phosphorylation domain within individual Ca-ATPase polypeptide chains.

Fluorescence Anisotropy Measurements of Phospholipid Acyl Chain Dynamics. Additional resolution of possible changes in the structure of membrane phospholipids resulting from the incorporation of LPC were obtained using frequency domain fluorescence spectroscopy to measure the excited-state lifetime and rotational dynamics of TMA-DPH partitioned into homogeneous vesicles made from either SR lipids or SR membranes. The excited-state lifetime of TMA-DPH is longer in native SR membranes (Table 5), suggesting that the presence of the Ca-ATPase alters the polarity near the bilayer surface. Furthermore, in agreement with previous observations we find that the Ca-ATPase functions to reduce the rotational mobility of membrane phospholipid acyl chains (*49*). These latter results are consistent with earlier suggestions that specific interactions between phospholipid headgroups and the Ca-ATPase are functionally important (*5*), and emphasize that these lifetime and anisotropy measurements are sensitive to changes in lipid−protein interactions. It is therefore significant that incorporation of LPC has essentially no effect on the average lifetime or rotational dynamics of TMA-DPH, irrespective of the presence of the Ca-ATPase (Table 5). These observations are furthermore consistent with measurements of the overall rotational dynamics of the Ca-ATPase (see above), which are unaffected by the incorporation of LPC (Table 4). Thus, LPC does not modify the structural dynamics (fluidity) of the phospholipid acyl chains.

Table 4: Rotational Dynamics of Er-ITC-Modified Ca-ATPase[a]

[LPC]/[SR] (mass/mass)	r_0	g_1	ϕ_1 (μs)	g_2	ϕ_2 (μs)	r_∞
0	0.34 (0.01)	0.58 (0.01)	6.4 (0.5)	0.18 (0.02)	170 (40)	0.08 (0.01)
0.2	0.34 (0.01)	0.52 (0.01)	7.4 (0.8)	0.28 (0.01)	170 (10)	0.07 (0.01)

[a] Experimental conditions are as described in the legend to Table 2. Indicated values represent averages of five independent measurements; standard errors of the mean are indicated in parentheses. Parameter values were obtained by fitting the data to the following equation: $A(t) = r_0\sum_i g_i e^{-t/\phi_i} + r_\infty$.

Table 5: Rotational Dynamics of TMA-DPH[a]

[LPC]/[SR] (mass/mass)	$\langle\tau\rangle$[b] (ns)	r_0	S	ϕ_1 (ns)	χ_R^2
	SR Lipids[c]				
0	4.1 ± 0.1	0.37 ± 0.01	0.70 ± 0.01	2.4 ± 0.2	1.5
0.2	4.2 ± 0.2	0.38 ± 0.01	0.69 ± 0.01	2.3 ± 0.1	0.8
	SR (Fast Exchange Model)[c]				
0	4.4 ± 0.2	0.39 ± 0.01	0.77 ± 0.01	1.8 ± 0.1	0.4
0.2	4.5 ± 0.3	0.39 ± 0.01	0.77 ± 0.01	1.7 ± 0.2	1.0
	SR (Protein-Associated Lipids Calculated Assuming Slow Exchange)[d]				
0	4.9 ± 0.3	0.39 ± 0.01	0.84 ± 0.01	1.0 ± 0.2	0.6
0.2	5.4 ± 0.3	0.39 ± 0.01	0.87 ± 0.01	0.8 ± 0.3	1.5

[a] Experimental conditions are as described in the legend to Table 2. Indicated values represent averages of two measurements assuming frequency-independent errors in the phase and modulation to be 0.2° and 0.005, respectively. Data were collected at 16 frequencies between 3 and 200 MHz; standard deviations are indicated in parentheses. [b] Average lifetime of TMA-DPH. [c] Parameter values were obtained by fitting the data to the equation $A(t) = r_0\sum_i g_i e^{-t/\phi_i} + r_\infty$, where $S = [r_\infty/r_0]^{0.5}$ assuming a homogeneous population of membrane phospholipids. [d] Parameter values for protein-associated lipids were calculated assuming slow exchange and that lifetime and rotational dynamics of the bulk lipids not in contact with the Ca-ATPase are identical to that observed in vesicles made from extracted SR lipids (see Experimental Procedures).

DISCUSSION

Summary of Results. Incorporation of nonsolubilizing concentrations of LPC into native SR membranes reduces

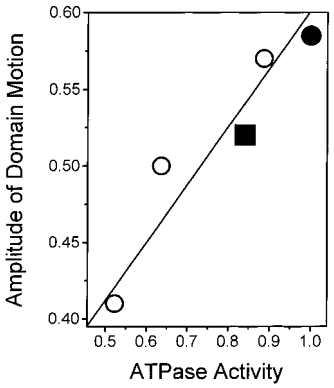

FIGURE 4: Correlation Between ATPase Activity and Rotational Dynamics of the Phosphorylation Domain. Amplitude of domain motion (i.e., g_1; see Table 4) and corresponding enzymatic activities for the Ca-ATPase in native SR membranes (●) and following the addition of 0.2 mg of LPC per milligram of SR protein (■). Data corresponding to the Ca-ATPase reconstituted into vesicles containing 0, 25, and 50 mol % phosphatidylethanolamine (○) are obtained from ref *5*.

the maximal transport rate of the Ca-ATPase without affecting (i) maximal coupling efficiency between ATP hydrolysis and calcium transport, (ii) apparent calcium affinity, or (iii) cooperative interactions between high-affinity calcium binding sites (Figure 2; Table 1). There are corresponding decreases in rotational mobility of the phosphorylation domain (Figure 3), suggesting the structural coupling between the nucleotide binding and phosphorylation sites in the cytosolic region and the spatially distant transmembrane helices in contact with membrane lipids. At the same time, LPC does not significantly alter either the rate of overall rotational motion of the Ca-ATPase with respect to the membrane normal or the lipid acyl chain rotational dynamics (Tables 4 and 5), indicating that interactions between neither Ca-ATPase polypeptide chains nor lipid fluidity are affected by LPC (*68*, *70*).

Lipid−Protein Interactions and Ca-ATPase Function. A similar relationship between catalytic function and the rotational dynamics of the phosphorylation domain is observed upon reconstitution of the Ca-ATPase in the presence of variable amounts of PE, which was altered between 0% and 50% (mol/mol) of the membrane phospholipids (*5*) (Figure 4). DOPE (50%) was found to be necessary to obtain rates of ATP hydrolysis that approximate that observed in native SR membranes (which contain 16% ± 4% PE; ref *59*) in these earlier experiments involving the reconstitution of affinity-purified Ca-ATPase with variable amounts of DOPE and DOPC (*5*), suggesting that this simple lipid composition can substitute for native SR lipids. Thus, increasing the amount of PE functions to *enhance* both enzymatic activity and the amplitude of rotational motion involving the phosphorylation domain of the Ca-ATPase. In contrast, addition of LPC to native SR membranes functions to *reduce* both enzymatic activity and the amplitude of domain motion. These results indicate that PE headgroups and LPC have opposite effects on enzymatic activity and the rotational dynamics of the phosphorylation domain of the Ca-ATPase, as is expected since they have opposite effects on membrane surface structure. However, the similar relationship between the amplitude of domain motion and the enzymatic activity of the Ca-ATPase suggests that a number of different membrane phospholipids can modulate catalytic function through changes in the structural dynamics of the phosphorylation domain (Figure 4). Furthermore, in a manner similar to LPC addition, different PE concentrations do not alter other dynamic structural properties of the Ca-ATPase or membrane fluidity. The amplitude of the phosphorylation domain motion has been previously suggested to be sensitive to the stiffness of the stalk region located proximal to the membrane surface, whose density is significantly altered by calcium binding (*16*, *17*). Thus, membrane phospholipids may function to modulate catalytically important motions normally involved in the transport cycle of the Ca-ATPase through the modification of protein structural elements critical to conformational coupling.

Relationship to Previous Studies. The fluidity of membrane phospholipids has previously been shown to constrain catalytically important motions associated with Ca-ATPase function (*72*−*75*). For example, the length of the phospholipid acyl chains must complement that of the transmembrane sequences of the Ca-ATPase in order to minimize hydrophobic mismatch and prevent aggregation between Ca-ATPase polypeptide chains (*76*−*77*). However, within liquid crystalline bilayers lipid fluidity is not a primary factor in determining enzyme function, as changes in phospholipid composition modulate Ca-ATPase function in a manner independent of acyl chain rotational dynamics (*78*−*79*). It has therefore been suggested that differences in the interactions between membrane phospholipids may modulate membrane protein function through changes in the lateral tension or elastic stress of the bilayer (*8*, *80*). Alternatively, interactions between specific membrane phospholipids and the Ca-ATPase have been suggested to be critical to the optimal function of a range of different membrane proteins, including the Ca-ATPase (*17*−*18*, *81*). However, the weak binding affinities of different membrane phospholipids to the Ca-ATPase are very similar irrespective of headgroup or acyl chain structure (*79*), suggesting essentially no selective binding interactions between membrane phospholipids and the Ca-ATPase. In contrast the membrane surface potential, which is sensitive to differences in the average conformation of membrane phospholipid headgroups relative to the membrane normal, is expected to be altered by the phospholipid headgroup composition (*13*, *24*, *43*).

Previous studies have shown that van der Waals contact interactions between phospholipid acyl chains function to constrain the cross-sectional area available to the phospholipid headgroup, which undergoes rapid rotational motion around the C(1)−C(2) bond of the glycerol backbone relative to the membrane normal; this rotational motion is essentially uncoupled from the slower rotational motion of the phospholipid acyl chains relative to the membrane normal (*43*, *82*, *83*). Therefore, the remarkable lack of effect on the dynamics of fatty acyl chains by either 20% (mass/mass) LPC in native SR or variations in PE content in reconstituted proteoliposomes suggests that primary effects of LPC on function are the result of changes in headgroup conformation and concomitant modifications of membrane surface potential. Membrane surface potential, in turn, has the potential to alter conformational barriers of catalytically important motions of the Ca-ATPase and thus modifying transport function (*22*−*26*, *84*, *85*).

Physiological Significance. The precise role of lysophospholipids in membrane signaling remains unclear, and may

involve the direct modulation of the functional properties of ion channels and electrogenic ion pumps (*86*−*90*). However, with the exception of gramicidin, whose oligomeric state is modulated by LPC, there is currently little structural information regarding the modulation of membrane protein function by LPC (*90*). In this respect, the Ca-ATPase represents both a model system for studies of LPC modulation of active transport as well as a potential cellular target of LPC. The structural coupling between LPC and the phosphorylation domain of the Ca-ATPase provides direct evidence that changes in membrane phospholipid composition can modulate the structure and function of membrane proteins. In addition, LPC itself may play a role in promoting cellular survival under conditions of oxidative stress mediated by the Ca-ATPase. For example, during ischemia and reperfusion in cardiomyocytes, reactive oxygen species (ROS) selectively oxidize highly unsaturated phospholipid acyl chains, which are primarily located at the *sn*-2 position of membrane phospholipids. Subsequent cleavage of the oxidatively modified fatty acyl chain by phospholipase A_2 (PLA_2) is modulated by intracellular calcium concentrations either directly or through calmodulin (*29*). Thus, the inhibition of the Ca-ATPase following generation of LPC under conditions of oxidative stress has the potential to prolong the activation of PLA_2 necessary for membrane remodeling by increasing the length of the calcium transient. Following the generation of LPC there is a substantial increase in PE levels (*30*, *32*, *91*), which has the potential to activate the Ca-ATPase through modulation of its phosphorylation domain and thus restoring calcium homeostasis (Figure 8) (*5*). Similar increases in PE levels have also been observed under other conditions of oxidative stress (i.e., chronic administration of ethanol) (*92*−*93*), suggesting that physiological changes in lipid composition resulting from a range of physiological stimuli may play an adaptive role in modulating intracellular calcium transients.

Conclusions and Future Directions. We have demonstrated a structural coupling between membrane phospholipid headgroups, the amplitude of the phosphorylation domain, and the transport function of the Ca-ATPase. Thus, changes in the composition of membrane phospholipids are expected to alter the transport activity of the Ca-ATPase and thereby modify the duration of calcium transients involved in cellular signaling mechanisms. Future studies should investigate whether there are correlated motions involving other domain elements within the Ca-ATPase that are modulated by physiological affecters of Ca-ATPase function.

REFERENCES

1. Hidalgo, C. (1987) *Crit. Rev. Biochem. 21*, 319−347.
2. Cortese, J. D., McIntyre, J. O., Duncan, T. M., and Fleischer, S. (1989) *Biochemistry 28*, 3000−3008.
3. Bhushan, A., and McNamee, M. G. (1993) *Biophys. J. 64*, 716−723.
4. Brown, M. F. (1994) *Chem. Phys. Lipids 73*, 159−180.
5. Hunter, G. W., Negash, S., and Squier, T. C. (1999) *Biochemistry 38*, 1356−1364.
6. Dalton, K. A., East, J. M., Mall, S., Oliver, S., Strarling, A. P., and Lee, A. G. (1998) *Biochem. J. 329*, 637−646.
7. Cullis, P. R., and de Kruijff, B. (1979) *Biochim. Biophys. Acta 559*, 399−420.
8. Gruner, S. M. (1985) *Proc. Natl. Acad. Sci. U.S.A. 82*, 3665−3669.
9. Sen, A., Yang, P. W., Mantsch, H. H., and Hui, S.-W. (1988) *Chem. Phys. Lipids 47*, 109−116.
10. Fenske, D. B., Jarrell, H. C., Guo, Y., and Hui, S. W. (1990) *Biochemistry 29*, 11222−11229.
11. Thurmond, R. L., Dodd, S. W., and Brown, M. F. (1991) *Biophys. J. 59*, 108−113.
12. Shin, T.-B., Leventis, R., and Silvius, J. R. (1991) *Biochemistry 30*, 7491−7497.
13. Ulrich, A. S., Sami, M., and Watts, A. (1994) *Biochim. Biophys. Acta 1191*, 225−230.
14. McIntosh, H. H. (1996) *Chem. Phys. Lipids 81*, 117−131.
15. MacLennan, D. H., Rice, W. J., and Green, N. M. (1997) *J. Biol. Chem. 272*, 28815−28818.
16. Ogawa, H., Stokes, D. L., Sasabe, H., and Toyoshima, C. (1998) *Biophys. J. 75*, 51−52.
17. Huang, S., and Squier, T. C. (1998) *Biochemistry 37*, 18064−18073
18. Navarro, J., Toivio-Kinnucan, M., and Racker, E. (1984) *Biochemistry 23*, 130−135.
19. Cheng, K. H., Lepock, J. R., Hui, S. W., and Yeagle, P. L. (1986) *J. Biol. Chem. 261*, 5081−5087.
20. Gould, G. W., McWhirter, J. M., East, J. M., and Lee, A. G. (1987) *Biochim. Biophys. Acta 904*, 36−44.
21. Schiffer, M., Chang, C.-H., and Stevens, F. J. (1992) *Protein Eng. (London) 5*, 213−214.
22. Flewelling, R. F., and Hubbell, W. L. (1986) *Biophys. J. 49*, 541−552.
23. Honig, B. H., Hubbell, W. L., and Flewelling, R. F. (1986) *Annu. Rev. Biophys. Biophys. Chem. 15*, 163−193.
24. Seelig, J., Macdonald, P. M., and Scherer, P. G. (1987) *Biochemistry 26*, 7535−7541.
25. Cevc, G. (1990) *Biochim. Biophys. Acta 1031*, 311−382.
26. Nieto-Frausto, J., Läuger, P., and Apell, H.-J. (1992) *Biophys. J. 61*, 83−95.
27. Rhee, S. G., and Dennis, E. A. (1996) in *Signal Transduction* (Heldin, C.-H., and Purton, M., Eds.) pp 173−188, Chapman & Hall, London, U.K.
28. Weiss, J. N. (1997) in *The Myocardium* (Langer, G. A., Ed.) pp 81−142, Academic Press, New York.
29. De Windt, L. J., Reneman, R. S., Van der Vusse, G. J., and Van Bilsen, M. (1998) *Mol. Cell. Biochem. 180*, 65−73.
30. Clements, M. P., Bliss, T. V. P., and Lynch, M. A. (1991) *Neuroscience 45*, 379−389.
31. Undrovinas, A. I., Fleidervish, I. A., and Makielski, J. C. (1992) *Circ. Res. 71*, 1231−1241.
32. Farooqui, A. A., Yang, H.-C., Rosenberger, T. A., and Horrocks, L. A. (1997) *J. Neurochem. 69*, 889−901.
33. Fernandez, J. L., Rosemblatt, M., and Hidalgo, C. (1980) *Biochim. Biophys. Acta 599*, 552−568.
34. Folch, J., Lees, M., and Sloane Stanley, G. H. (1957) *J. Biol. Chem. 226*, 497−509.
35. Hidalgo, C., Ikemoto, N., and Gergely, J. (1976) *J. Biol. Chem. 251*, 4224−4232.
36. Huang, S., Negash, S., and Squier, T. C. (1998) *Biochemistry 37*, 6949−6957.
37. Mitchinson, C., Wilderspin, A. F., Trinnaman, B. J., and Green, N. M. (1982) *FEBS Lett. 146*, 87−92.
38. Schaffner, W., and Weissman, C. (1973) *Anal. Biochem. 56*, 502−514.
39. Hunter, G. W. (1997) Doctoral dissertation, page 38, The University of Kansas, Lawrence, KS.
40. Karon, B. S., Nissen, E. R., Voss, J., and Thomas, D. D. (1995) *Anal. Biochem. 227*, 328−333.
41. Lanzetta, P. A., Alverez, L. J., Reinsch, P. S., and Candia, O. (1979) *Anal. Biochem. 100*, 95−97.
42. Pedigo, S., and Shea, M. (1995) *Biochemistry 34*, 1179−1196.
43. Hunter, G. W., and Squier, T. C. (1998) *Biochim. Biophys. Acta 1415*, 63−76.
44. Eads, T. M., Thomas, D. D., and Austin, R. H. (1984) *J. Mol. Biol. 179*, 55−81.
45. Weber, G. (1981) *J. Phys. Chem. 85*, 949−953.
46. Lakowicz, J. R., Cherek, H., Maliwal, B. P., and Gratton, E. (1985) *Biochemistry 24*, 376−383.

47. Beechem, J. M., Gratton, E., Ameloot, M., Knutson, J. R., and Brand, L. (1991) *Topics in Fluorescence Spectroscopy* (Lakowicz, J. R., Ed.) Vol. 2, pp 241−306, Plenum Press, New York.
48. Johnson, M. L., and Faunt, L. M. (1992) *Methods Enzymol. 210*, 1−37.
49. Squier, T. C., and Thomas, D. D. (1989) *Biophys. J. 56*, 735−748.
50. Weber, G., and Daniel, E. (1966) *Biochemistry 5*, 1900−1907.
51. Squier, T. C., Bigelow, D. J., Garcia de Ancos, J., and Inesi, G. (1987) *J. Biol. Chem. 262*, 4748−4754.
52. Highsmith, S., and Cohen, J. A. (1987) *Biochemistry 26*, 154−161.
53. Bigelow, D. J., and Inesi, G. (1991) *Biochemistry 30*, 2113−2125.
54. Runnels, L. W., and Scarlata, S. F. (1995) *Biophys. J. 69*, 502−514.
55. Yonekura, K., Stokes, D. L., Sasabe, H., and Toyoshima, C. (1997) *Biophys. J. 72*, 997−1005.
56. Blackman, S. M., Piston, D. W., and Beth, A. H. (1998) *Biophys. J. 75*, 1117−1130.
57. Lakowicz, J. R. (1983) *Principles of Fluorescence Spectroscopy*, Plenum Press, New York.
58. Brown, S. D., Baker, B. L., and Bell, J. D. (1993) *Biochim. Biophys. Acta 1168*, 13−22.
59. Bigelow, D. J., Squier, T. C., and Thomas, D. D. (1986) *Biochemistry 25*, 194−202.
60. Frond, R. J., East, J. M., Jones, O. T., and Lee, A. G. (1986) *Biochemistry 25*, 7544−7552.
61. Bigelow, D. J., and Inesi, G. (1992) *Biochim. Biophys. Acta 1113*, 323−338.
62. Inesi, G. (1994) *Biophys. J. 66*, 554−560.
63. Møller, J. V., Juul, B., and le Maire, M. (1996) *Biochim. Biophys. Acta 1286*, 1−51.
64. Dupont, Y., Guillain, F., and Lacapere, J. J. (1988) *Methods Enzymol. 157*, 206−219.
65. Squier, T. C., Bigelow, D. J., Ferdandez-Belda, F. J., de Meis, L., and Inesi, G. (1990) *J. Biol. Chem. 265*, 13713−13720.
66. Lee, A. G., Starling, A. P., Ding, J., East, J. M., and Wictome, M. (1994) *Biochem. Soc. Trans. 22*, 821−826.
67. Gryczynski, I., Wiczk, W., Inesi, G., Squier, T., and Lakowicz, J. R. (1989) *Biochemistry 28*, 3490−3498.
68. Fajer, P., Knowles, P. F., and Marsh, D. (1989) *Biochemistry 28*, 5634−5643.
69. Birmachu, W., and Thomas, D. D. (1990) *Biochemistry 29*, 3904−3914.
70. Cherry, R. J. (1992) in *The Structure of Biological Membranes* (Yeagle, P., Ed.) pp 507−537, CRC Press, Boca Raton, FL.
71. Thomas, D. D., and Mahaney, J. E. (1993) in *Protein−Lipid Interactions* (Watts, A., Ed.) Elsevier Science Publishers B. V., North-Holland.
72. Moore, B. M., Lentz, B. R., and Meissner, G. (1978) *Biochemistry 17*, 5248−5255.
73. Almeida, L. M., Vaz, W. L. C., Zachariasse, K. A., and Madeira, V. M. C. (1982) *Biochemistry 21*, 5972−5977.
74. Bigelow, D. J., Squier, T. C., and Thomas, D. D. (1986) *Biochemistry 25*, 194−202.
75. Squier, T. C., Bigelow, D. J., and Thomas, D. D. (1988) *J. Biol. Chem. 263*, 9178−9186.
76. Johannsson, A., Keightley, C. A., Smith, G. A., Richards, C. D., Hesketh, T. R., and Metcalfe, J. C. (1981) *J. Biol. Chem. 256*, 1643−1650.
77. Cornea, R. L., and Thomas, D. D. (1994) *Biochemistry 33*, 2912−2920.
78. East, J. M., Jones, O. T., Simmonds, A. C., and Lee, A. G. (1984) *J. Biol. Chem. 259*, 8070−8071.
79. Lee, A. G., Dalton, K. A., Duggleby, R. C., East, J. M., and Starling, A. P. (1995) *Biosci. Rep. 15*, 289−298.
80. Gruner, S. M. (1989) *J. Phys. Chem. 93*, 7562−7570.
81. Hidalgo, C., Petrucci, D. A., and Vergara, C. (1982) *J. Biol. Chem. 257*, 208−216.
82. Lewis, R. N. A. H., and McElhaney, R. N. (1992) in *The Structure of Biological Membranes* (Yeagle, P., Ed.) pp 73−155, CRC Press, Boca Raton, FL.
83. Yeagle, P. (1993) in *The Membranes of Cells*, Academic Press, New York.
84. Levy, D., Seigneuret, M., Bluzat, A., and Rigaud, J. L. (1990) *J. Biol. Chem. 265*, 19524−19534.
85. Hao, M. H., and Harvey, S. C. (1995) *Biochim. Biophys. Acta 1234*, 5−14.
86. Shull, G. E., Schwartz, A., and Lingrel, J. B. (1985) *Nature 316*, 691−695.
87. Oishi, K., Zheng, B., and Kuo, J. F. (1990) *J. Biol. Chem. 265*, 70−75.
88. Mock, T., and Man, R. Y. K. (1990) *Lipids 25*, 357−362.
89. Burnashev, N. A., Undrovinas, A. I., Fleidervish, I. A., Makielski, J. C., and Rosenshtraukh, L. V. (1991) *J. Mol. Cell. Cardiol. 23*, 23−30.
90. Lundbaek, J. A., and Andersen, O. S. (1994) *J. Gen. Physiol. 104*, 645−673.
91. Horid'ko, T. M., Marhitych, V. M., Klimashevs'kyi, V. M., Hovseiveva, N. M., Puhach, B. V., Hula, N. M., and Frol'kis, V. V. (1996) *Ukr. Biokhim. Zh. (Ukraine) 68*, 99−102.
92. Kuwahara, Y., Yanagishita, T., Konno, N., and Katagiri, T. (1997) *Basic Res. Cardiol. 92*, 214−222.
93. Lieber, C. S. (1997) *Adv. Pharmacol. 38*, 601−628.

BI982392G